

A comprehensive high Reynolds number effects simulation method for wind pressures on cooling tower models

X.X. Cheng^{1,2}, L. Zhao¹, Y.J. Ge^{*1}, J. Dong² and C. Demartino²

¹State Key Laboratory for Disaster Reduction in Civil Engineering, Tongji University, Shanghai 200092, China

²College of Civil Engineering, Nanjing Tech University, Nanjing 211816, China

(Received July 19, 2016, Revised November 26, 2016, Accepted November 28, 2016)

Abstract. The traditional method for the simulation of high Reynolds number (Re) effects on wind loads on cooling tower models in wind tunnels focuses only on the mean wind pressure distribution. Based on observed effects of some key factors on static/dynamic flow characteristics around cooling towers, the study reported in this paper describes a comprehensive simulation method using both mean and fluctuating wind pressure distributions at high Re as simulation targets, which is indispensable for obtaining the complete full-scale wind effects in wind tunnels. After being presented in this paper using a case study, the proposed method is examined by comparing the full covariance matrices and the cross-spectral densities of the simulated cases with those of the full-scale case. Besides, the cooling tower's dynamic structural responses obtained using the simulated wind pressure fields are compared with those obtained by using the full-scale one. Through these works, the applicability and superiority of the proposed method is validated.

Keywords: cooling tower; wind tunnel model test; Reynolds number effect; mean/fluctuating wind pressure distribution; field measurement

1. Introduction

A lot of works have proven that fluid flows around bluff bodies largely depend on the Reynolds number (Re), including flows around semi-aerodynamic bodies (Roshko 1961, Achenbach 1968, Bearman 1969, Farell and Blessmann 1983, Qiu, Sun *et al.* 2014a, Qiu, Sun *et al.* 2014b, Ma, Liu *et al.* 2015) and those around non-aerodynamic bodies (Lee, Kwon *et al.* 2014, Kargarmoakhar, Chowdhury *et al.* 2015, Wang and Gu 2015). Thus, the difference in Re between the wind tunnel test of an object and the full-scale situation results in different flow characteristics, which can cause inaccuracies in the wind tunnel simulations. Fortunately, Re is not the only factor that influences the fluid flow. Surface roughness of the test body is also an important influence. And it is widely acknowledged that at a high Re the mean wind pressure distribution around a circular cylinder can be reproduced at lower values of Re with a suitable roughening of the surface of the round body (Lawson 1982). This method (hereinafter referred to as the traditional method) has been used for decades for simulating high Re effects on circular cylinder structural models in wind tunnel experiments.

*Corresponding author, Professor, E-mail: yaojunge@tongji.edu.cn

As typical circular cylinders, same situation holds true for wind tunnel model tests on cooling towers. Adopting the traditional Re effect simulation method, the mean wind pressure distribution based on field measurements at high Re is used as the simulation target. Generally, after some attempts of different surface roughness, the simulation process will be completed when getting the case whose mean wind pressure distribution overlaps the target. Undoubtedly, the static wind effects obtained accordingly is accurate. However, the simulation results are typically not checked for another important aspect of flow characteristics, i.e., fluctuating wind pressure distribution. This is chiefly due to the less reasonable assumption that the mean wind pressure distribution represents the entire flow state. In reality, the mean wind pressure distribution is only one aspect of flow characteristics, and even when it is simulated accurately for a test, the produced flow might still deviate from the full-scale state in view of other characteristics based on our experiences. In this regard, an improvement for higher simulation veracity should be attempted by introducing other aspects of flow characteristics into the Re effects simulation process, e.g., the fluctuating wind pressure distribution. It is believed that enriching the number of simulation targets can effectively mitigate the underlying problem with the traditional Re effects simulation.

As mentioned, for cooling tower wind tunnel model tests, surface roughness adjustment is generally used as the accepted approach for simulation. As the number of simulation targets increases, the simulation method requires improvement. In addition, it has been proved that the surface roughness of the sample body and the turbulence intensity of the incoming flow both influence the flow characteristics around a sample body (Niemann and Hölscher 1990). However, the surface roughness is generally used as the sole measure of the Re effect simulation. The possibility of including turbulence intensity in the simulation should also be discussed.

In view of this narrative, this study develops a novel simulation method based on the study of multiple effects on the mean/fluctuating wind pressure distributions on cooling towers. The proposed method is demonstrated using data from a full-scale case study. Then the effectiveness of the new method is verified according to two approaches. The first approach is to compare the simulated covariance matrices and cross-spectral densities to the full-scale ones. The second approach involves comparison of the cooling tower's dynamic structural responses obtained using the simulated wind pressure field with the responses obtained for the full-scale cooling tower.

2. Effects of key factors on static/dynamic flow characteristics

In this portion of the study, the effects of three key factors, i.e., Re, surface roughness and turbulence intensity, on both mean and fluctuating wind pressure distributions are individually examined. These analyses lay a foundation for the proposed comprehensive Re effects simulation method as detailed below.

2.1 Re effects

Generally, the difference in the Re between the wind tunnel test and the full-scale case for cooling towers is around two or three orders of magnitude, which would cause notable differences in the mean/fluctuating wind pressure distributions. In this section, comparisons of mean/fluctuating wind pressure distributions under different Re are conducted to demonstrate such effects.

The mean/fluctuating wind pressure distributions with a low Re are obtained using a wind

tunnel test. The wind tunnel test is conducted in the TJ-3 atmospheric boundary layer (ABL) wind tunnel located at Tongji University in Shanghai. The wind tunnel is a closed circuit rectangular cross-section wind tunnel with a test section that is 15 m wide, 2 m high and 14 m long. The test wind speed can be continuously controlled in the 1.0 to 17.6 m/s range. The non-uniformity of the wind speed of the flow field in the test zone is less than 1%, the turbulence intensity is less than 0.5% and the average flow deviation angle is less than 0.5° . Using spires and ground roughness blocks, the flow field of Type B according to Ministry of Energy, P.R.C. (1989), i.e., the countryside open terrain, is simulated (see Fig. 1). In Fig. 1(a), the power spectral density is measured at 1 m height, and the simulated turbulence integral scale at that height is around 0.3 m.

The 1:200 pressure measuring cooling tower model that is used, is made of synthetic glass, which ensures its strength and rigidity. The cooling tower is equipped with 432 measurement points, 12×36 along the meridian and circumferential directions, respectively. The model and the distribution of the measuring points are shown in Fig. 2.

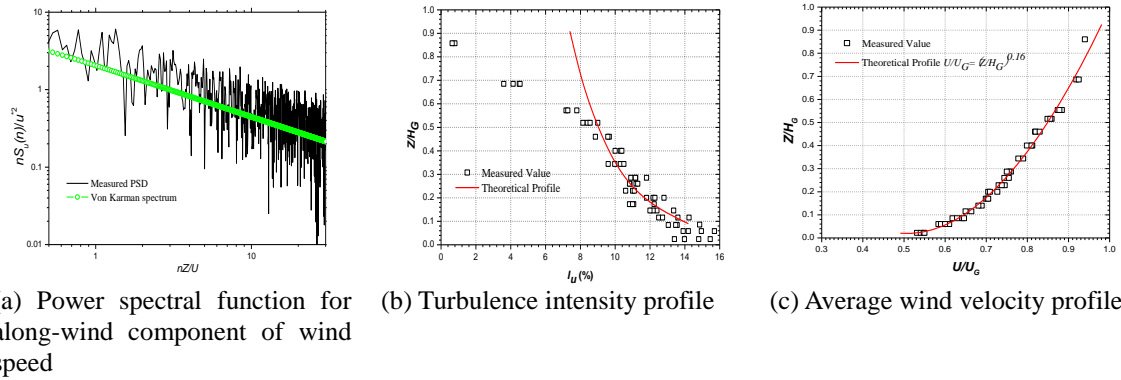
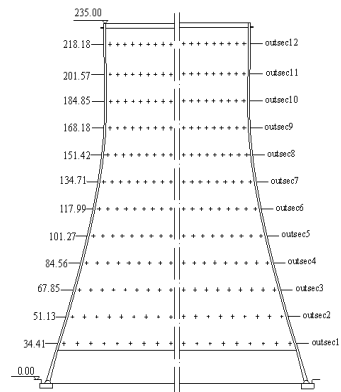


Fig. 1 Type B flow field in the TJ-3 (H_G and U_G refer to the gradient height and the geostrophic velocity, respectively)



(a) The cooling tower model in Type B flow field



(b) Layout of measuring points on the cooling tower model (the data represent the full-scale heights, unit: m)

Fig. 2 Cooling tower model and measuring points

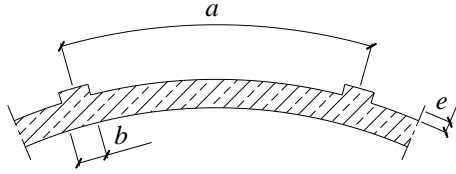


Fig. 3 Schematic diagram of relative roughness definition

To facilitate comparison with full-scale results obtained on cooling towers of various surface roughness, compressively varied surface roughness is set up on the model in wind tunnel tests. The relative roughness k of the model is defined as

$$k = \frac{e}{a} \quad (1)$$

As shown in Fig. 3, a corresponds to the rib spacing between the neighboring rough zones, b represents the width of the rough zone, and e is the thickness of the rough zone. Eq. (1) does not take rib width b into account, because it has been found from our previous tests that b is not a significant influence on the wind effects when a is relatively small.

The relative roughness of the model surface in different cases is shown in Table 1 and the Re numbers for both the prototype tower and the tower model under various wind speeds is shown in Table 2. As can be seen, there were 8 types of surface roughness and 4 types of wind speed, corresponding to a total of 32 (8×4) cases.

The dimensionless pressure coefficient at measure point i is defined as

$$C_{pi}(t) = \frac{P_i(t) - P_\infty(t)}{P_0(t) - P_\infty(t)} \quad (2)$$

where $P_i(t)$ is the pressure at measure point i at time t ; $P_0(t)$ and $P_\infty(t)$ are the total and the static reference pressures of the undisturbed flow at the height of measure point i at time t , respectively, which are measured using a Pitot tube located at an upstream position.

Table 1 Relative roughness for different cases

Type	Smooth	Single-layer r paper tape	Two-layer paper tape	Three-layer paper tape	Four-layer paper tape	1 × 0.5 thread	1 × 1 thread	1 × 2 thread
b (mm)	0	12	12	12	12	1	1	1
a (mm)*	1,645.9	45.7	45.7	45.7	45.7	45.7	45.7	45.7
e (mm)	0	0.1	0.2	0.3	0.4	0.5	1.0	2.0
k	0	2.19×10^{-3}	4.38×10^{-3}	6.56×10^{-3}	8.75×10^{-3}	10.9×10^{-3}	21.9×10^{-3}	43.8×10^{-3}

* Note: a is measured at throat height.

Table 2 Re number for full-scale and wind tunnel tests

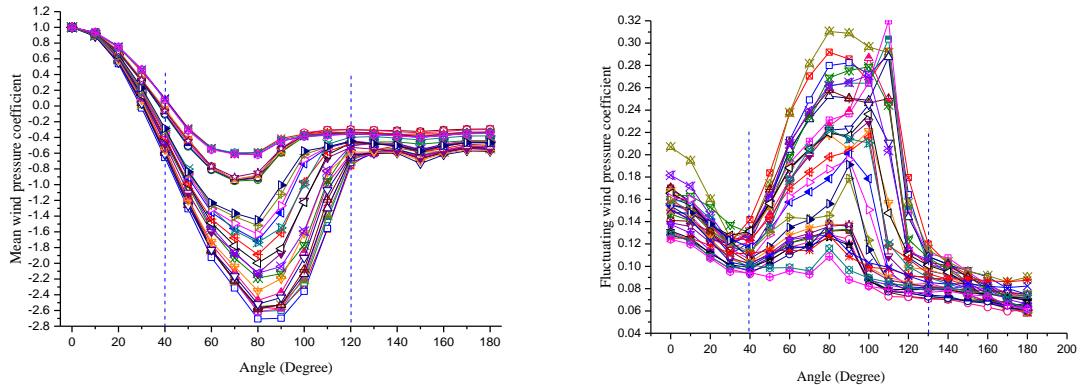
Wind speed (m/s)	Throat section diameter		Throat section diameter	
	of the prototype tower (m)	Re (prototype)	of the tower model (m)	Re (model)
6	104.78	4.19×10^7	0.5239	2.10×10^5
8	104.78	5.59×10^7	0.5239	2.79×10^5
10	104.78	6.99×10^7	0.5239	3.49×10^5
12	104.78	8.38×10^7	0.5239	4.19×10^5

The mean and fluctuating wind pressure coefficients are defined respectively as

$$C_{Pi} = \frac{\sum_{t=1}^n C_{Pi}(t)}{n} \quad (3)$$

$$C_{Pi_RMS} = \left(\frac{\sum_{t=1}^n (C_{Pi}(t) - C_{Pi})^2}{n} \right)^{1/2} \quad (4)$$

in which, $n=6000$ is the amount of data produced by one measuring point in each 1-min run (the sampling frequency is 100 Hz). To avoid the edge effects, the eighth section, which is close to the throat in the middle of the cooling tower model, is chosen as the study section. After wind tunnel tests for each case, the data obtained on the study section are processed using Eqs. (2)-(4) in turn to yield the mean/fluctuating wind pressure distributions (see Fig. 4). It is noteworthy that results presented in Fig. 4 not only facilitate the study of Re effects, but also suggest an improved high Re effects simulation method for wind tunnel tests (see Sec. 2.2).



(a) Mean wind pressure distribution

(b) Fluctuating wind pressure distribution

Fig. 4 Circumferential distributions of the wind pressure coefficient in Type B flow field

Table 3 Specifics for early full-scale measurement campaigns

	Tower name	Researcher	Location	Height	Height of measurement section	Surroundings	Relative surface roughness	Reynolds number
1	Weisweiler	Niemann (1971); Niemann and Propper (1975/1976)	Germany	104 m	62.53 m	A single tower surrounded by large buildings	6.5E-3	6.5E7
2	Martin's Creek	Sollenberger and Scanlan (1974)	U.S.A.	127 m	107.6 m	Two grouped towers	2.2E-2	1.0E8
3	(unknown)	Ruscheweyh (1975/1976)	Germany	114 m	Three sections along height	Four grouped towers	2E-3	6E7
4	Schmehausen	Niemann and Ruhwedel (1980)	Germany	122 m	55 m	A single tower	2.3E-2	4~6E7
5	(unknown)	Pirner (1982)	Czech	120 m	Five sections along height	(unknown)	Smooth	(unknown)
6	Maoming	Sun and Zhou (1983)	China	90 m	50 m	A single tower surrounded by large buildings	Smooth	5.4E7

Results with a high Re are obtained by field measurements. The specifics about the field measurement campaigns in history are described in Table 3. As can be seen from Table 3, the earliest-reported field measurement of mean wind pressure distribution is conducted on the Weisweiler cooling tower (Niemann 1971). The relative roughness k of the Weisweiler cooling tower is 6.5×10^{-3} , which is equal to that of the three-layer paper tape case in wind tunnel tests (see Table 1). Consequently, the result of the three-layer paper + 12 m/s wind speed case is selected for comparison to the results for the Weisweiler tower (see Fig. 5(a)). Because the surface roughness is identical and the oncoming flow is ABL turbulent flow in both cases, the variations are mainly due to the Re . From Fig. 5(a), the differences between the two curves appear to be significant. First, absolute values of pressure coefficients over the entire negative pressure zone are larger for the model than for the Weisweiler tower. For example, the minimum negative pressure coefficient for wind tunnel test is -1.7, while for Weisweiler it is -1.3. The pressure coefficients in the wake zone for the wind tunnel test are around -0.5, while those for Weisweiler are around -0.38. Second, the discrepancies in the occurrence positions of the minimum negative pressure and the flow separation are both around 10 degrees.

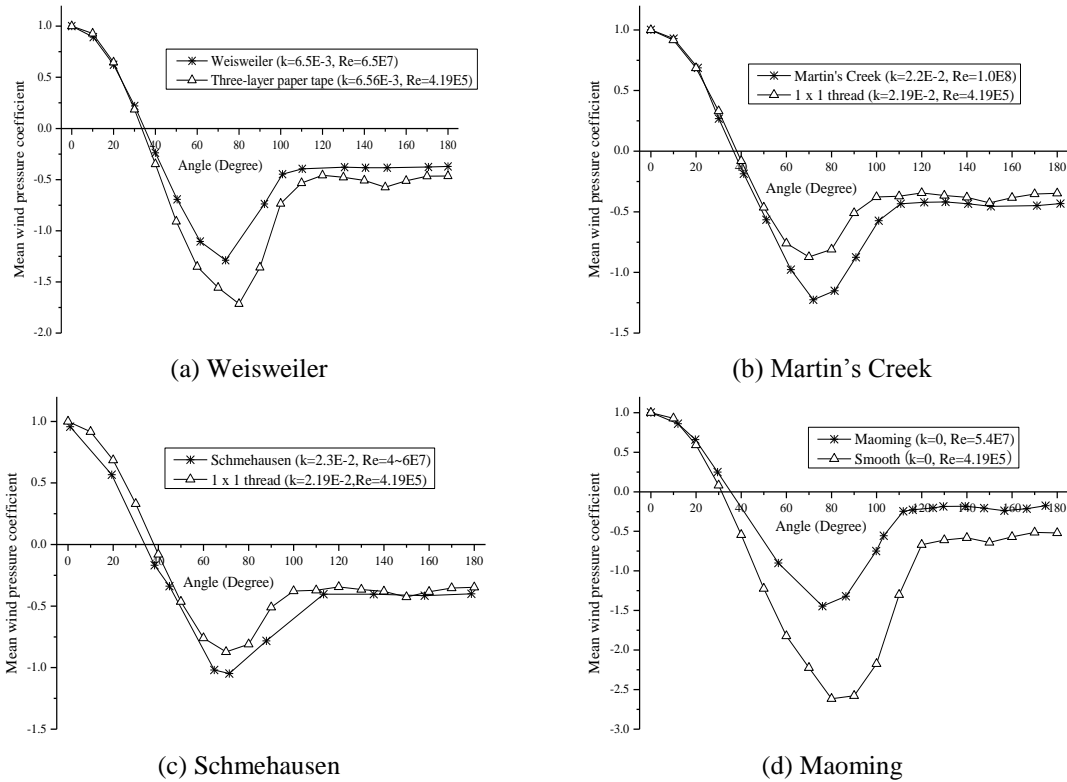
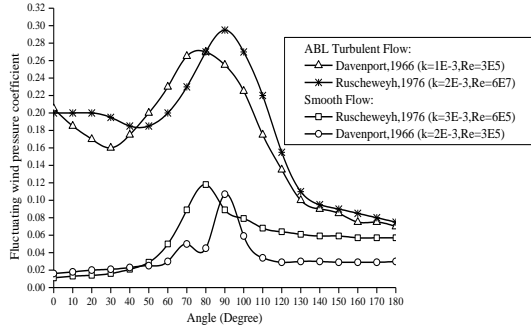


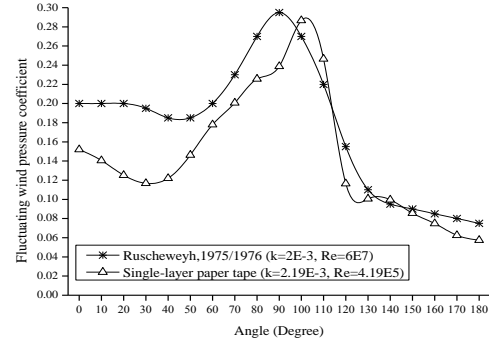
Fig. 5 Mean wind pressure distributions measured at the throats of four full-scale cooling towers and their corresponding wind tunnel results

Comparison between the fluctuating wind pressure distributions with different Re have been previously reported by Ruscheweyh (1975/1976), which is shown in Fig. 6(a). Comparing the field measurement fluctuating wind pressure distribution to the wind tunnel test result with turbulent flow in Fig. 6(a) (the two curves on the top), it can be seen that these results are quite similar. However, the relative roughness of the full-scale tower is twice that of the model tower, which makes this comparison less persuasive.

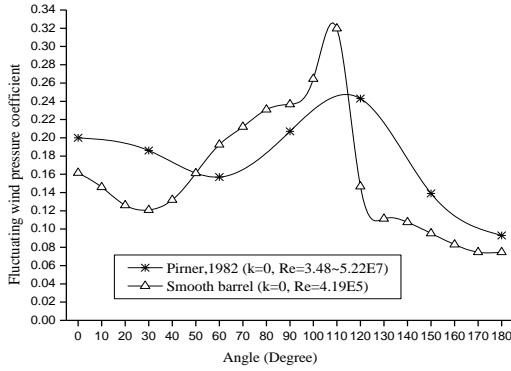
In Fig. 6(b), this paper compares the field measurement results of Ruscheweyh (1975/1976) with those of the wind tunnel test with a 12 m/s wind speed and the same relative roughness. As shown, there is some variation between the two curves which is not the case in Fig. 6(a). From 100 to 180 degrees, the two cases agree. However, from 0 to 90 degree, the fluctuating wind pressure coefficients of wind tunnel tests are much smaller than those of field measurements. Similar comparisons are made in Figs. 6(c) and 6(d). According to Figs. 6(c) and 6(d), field measurement results of Pirner (1982) and Niemann and Propper (1975/1976) are both notably different from their corresponding wind tunnel simulation results. It can be concluded from these facts that the Re effects on fluctuating wind pressure distribution are as significant as those on mean wind pressure distribution. Measures should be adopted to mitigate the Re effects on mean and fluctuating wind pressure distributions at the same time in the wind tunnel test.



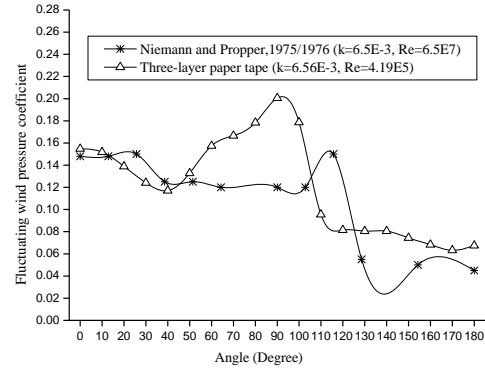
(a) Ruscheweyh's comparison (reprinted from Ruscheweyh (1975/1976))



(b) Ruscheweyh (1975/1976)



(c) Pirner (1982)



(d) Niemann and Propper (1975/1976)

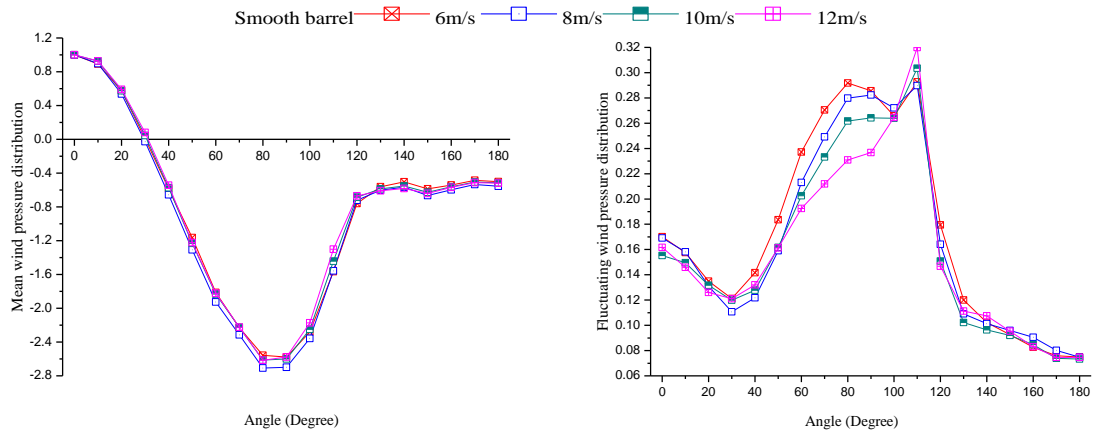
Fig. 6 Fluctuating wind pressure distributions measured at the throats of three full-scale cooling towers and the wind tunnel results

2.2 Surface roughness effects

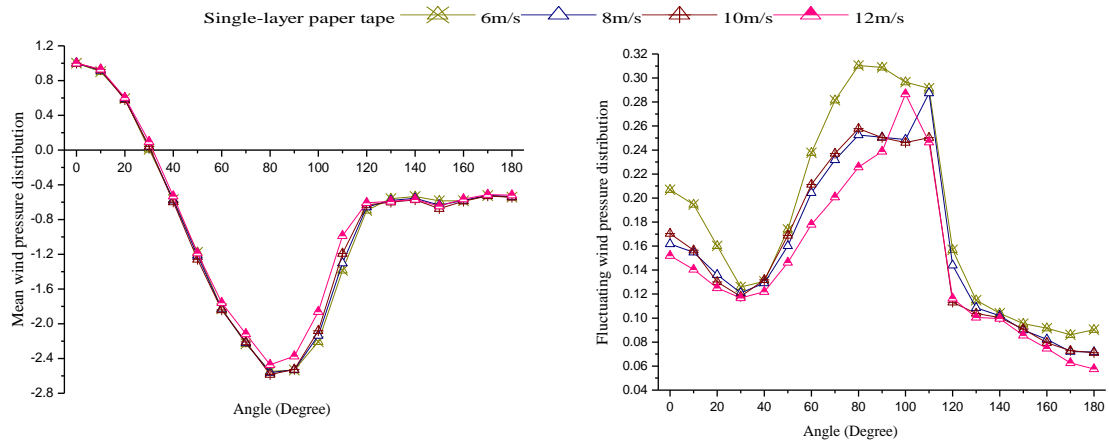
As is shown in Fig. 4, surface roughness effects on the mean and the fluctuating wind pressure distributions are both significant at a low Re , especially within the range from 40 to 120/130 degrees. This appears to indicate that surface roughness is an effective way to compensate for Re effects in wind tunnel tests. However, it appears to be difficult to compensate for two influences (the mean and fluctuating wind pressure distributions) using only one simulation measure.

To solve this problem, a careful analysis of all the curves shown in Fig. 4 is attempted. First, Fig. 4 is divided into many subfigures as shown in Fig. 7 based on the tower's surface roughness. In Figs. 7(a), 7(c), 7(e), 7(g), 7(i), 7(k), 7(m), 7(o), it appears that, in most cases, the mean wind pressure distribution curves for the tower with the same surface roughness, but varying wind velocity completely coincide. A similar situation doesn't appear in Figs. 7(b), 7(d), 7(f), 7(h), 7(j), 7(l), 7(n), 7(p), indicating that the variability of the fluctuating wind pressure distribution is stronger than that of the mean wind pressure distribution. This further suggests that, occasionally,

an effective simulation of a full-scale mean wind pressure distribution is not unique, but simulation of the corresponding real fluctuating wind pressure distribution might be unique. Thus, a two-step comprehensive Re effects simulation method for both mean and fluctuating wind pressure distributions is formulated (hereinafter referred to as the proposed method). First, all of the simulated mean wind pressure distributions are compared to a real case and all the situations where the mean wind pressure distribution coincides with the real case are selected. Second, within the selected case group, the fluctuating wind pressure distributions are further compared to the real case to determine the optimum simulation condition.

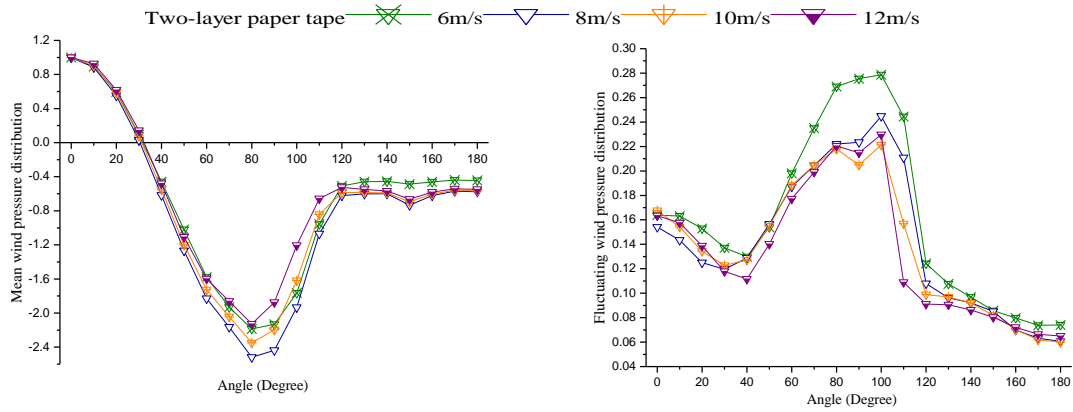


(a) Mean wind pressure distribution for smooth barrel case (b) Fluctuating wind pressure distribution for smooth barrel case



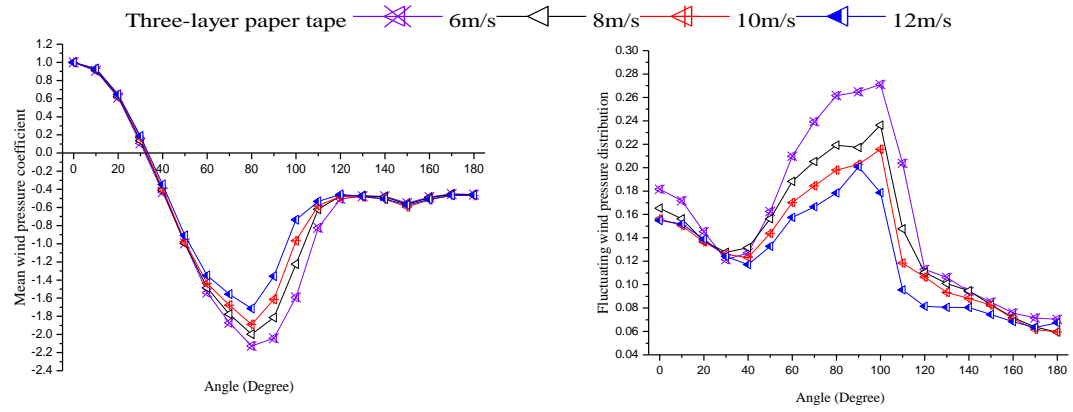
(c) Mean wind pressure distribution for single-layer paper tape case (d) Fluctuating wind pressure distribution for single-layer paper tape case

Continued-



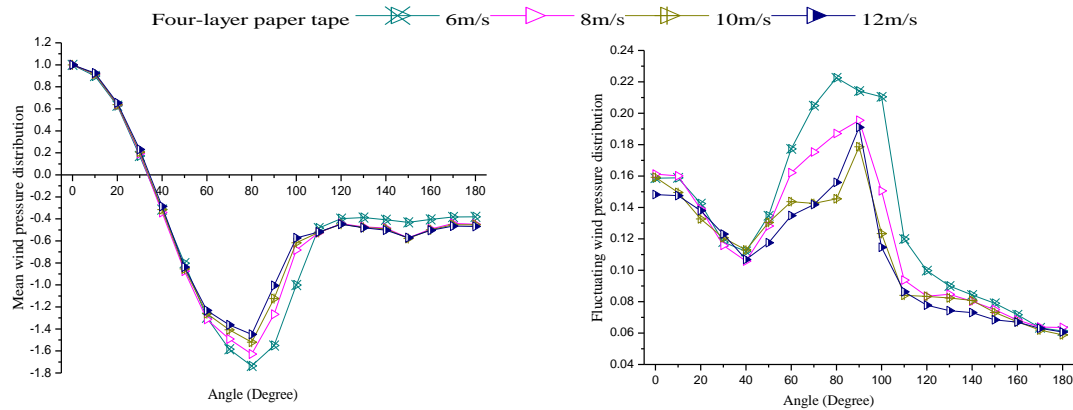
(e) Mean wind pressure distribution for two-layer paper tape case

(f) Fluctuating wind pressure distribution for two-layer paper tape case



(g) Mean wind pressure distribution for three-layer paper tape case

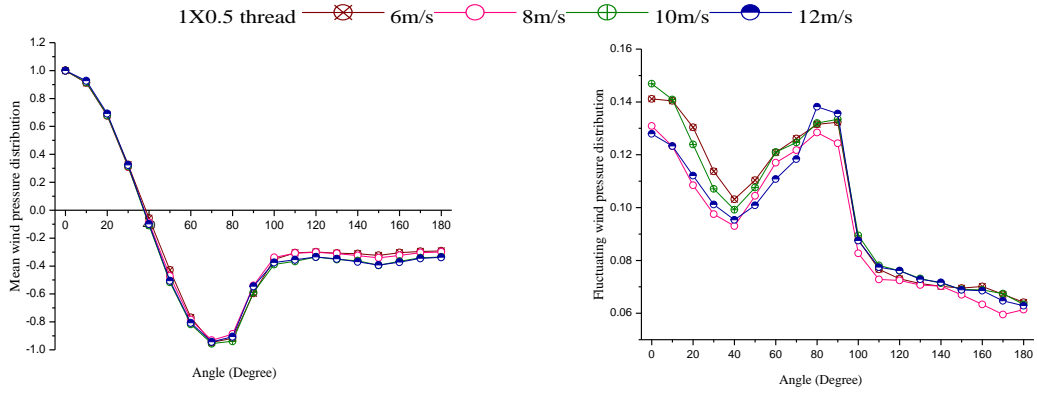
(h) Fluctuating wind pressure distribution for three-layer paper tape case



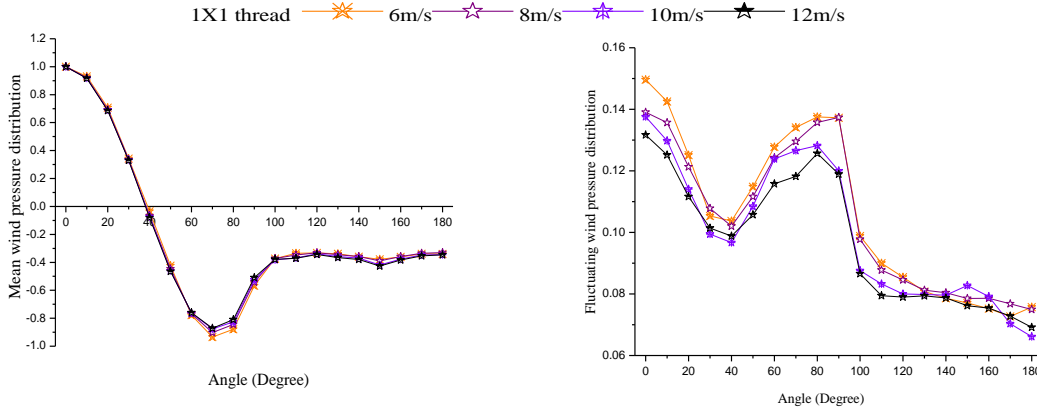
(i) Mean wind pressure distribution for four-layer paper tape case

(j) Fluctuating wind pressure distribution for four-layer paper tape case

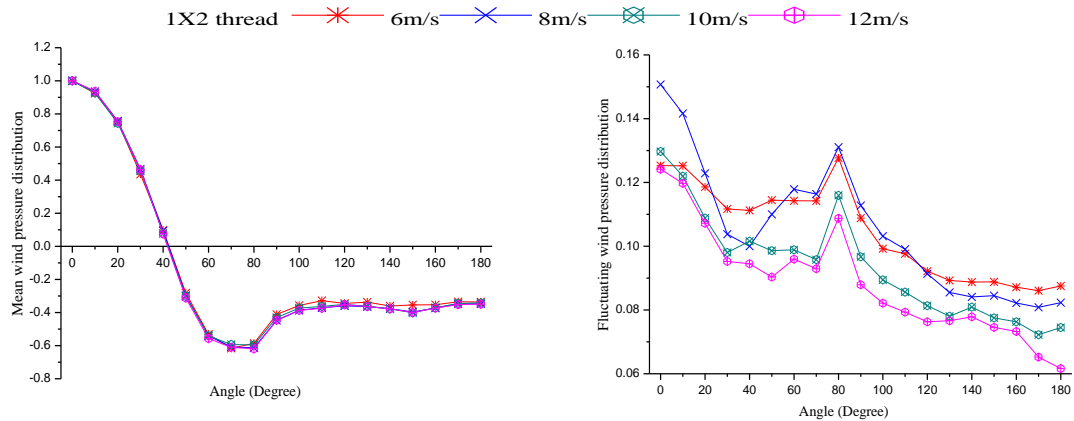
Continued-



(k) Mean wind pressure distribution for 1X0.5 thread case (l) Fluctuating wind pressure distribution for 1X0.5 thread case



(m) Mean wind pressure distribution for 1X1 thread case (n) Fluctuating wind pressure distribution for 1X1 thread case



(o) Mean wind pressure distribution for 1X2 thread case (p) Fluctuating wind pressure distribution for 1X2 thread case

Fig. 7 Circumferential distributions of the wind pressure coefficient in Type B flow field for different surface roughness cases

2.3 Turbulence intensity effects

Cheng, Zhao *et al.* (2015) has investigated the effects of the turbulence intensity on the mean/fluctuating wind pressure distributions using wind tunnel tests. The results demonstrate that the turbulence intensity effects on the fluctuating wind pressure distribution are significant (as also displayed in Fig. 6(a)), while the effects on the mean wind pressure distributions are insignificant. This helps to explain why most full-scale mean wind pressure distributions are similar (see Fig. 14(a)), but there are notable differences among the various full-scale fluctuating wind pressure distributions (see Fig. 14(b)).

In a traditional wind tunnel, turbulence is passively generated using spires and roughness elements, but it is difficult to control the flow characteristics using the traditional technique. In a multiple fan active control wind tunnel, continuously varying air flow turbulence intensity can be produced while maintaining the other environmental parameters (Pan, Zhao *et al.* 2011). Future use of active control wind tunnels will allow for another comprehensive high Re effects simulation method for cooling tower model tests. Such a test would consist of first, simulating the high Re effect on mean wind pressure distribution by adjusting the model surface roughness; second, simulating the high Re effect on fluctuating wind pressure distribution by adjusting the turbulence intensity of the trained flow. The new method requires substantial validation, which is not available for this study, but will be investigated in the future when an actively controlled wind tunnel can be employed to verify this method.

It should be noted that laminar air flow is used in some of the conducted wind tunnel model tests. As a result, the resulting dynamic wind effects may not accurately reflect the realistic situation (e.g., the two curves on the downside in Fig. 6(a)) and should not be utilized. In other words, modeling ABL in a wind tunnel is the precondition of accurate simulation of dynamic wind effects on cooling towers.

3. A case study: Peng-cheng cooling tower

To determine the applicability of the simulation method proposed in Sec. 2.2, an actual large hyperbolic cooling tower is used as the engineering background for a case study. Mean and fluctuating wind pressure distributions on the cooling tower are measured simultaneously and used as the simulation targets. Using wind tunnel test data presented in Fig. 4, the proposed method is demonstrated.

3.1 Setup for full-scale measurements

The 167-meter high smooth-walled cooling tower located in Peng-cheng electric power plant, Xu-zhou, China is chosen for field measurements. To its south, there is an adjacent cooling tower same size as the one for measurements, and there is an industrial complex to its west (see Fig. 8). However, to its north and east, there is no large interfering building and the upstream terrain is smooth. So, when the upcoming flows are from east or north, the measuring tower can be regarded as an isolated cooling tower. During its construction, 36 transducers are evenly installed around the tower's throat section at 130-meter high (see Figs. 9 and 10).

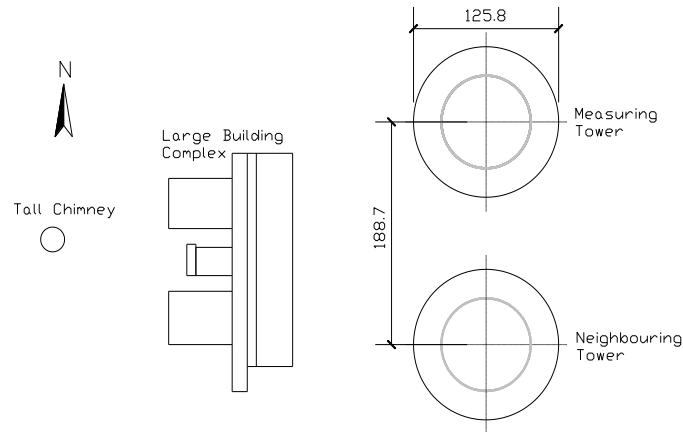


Fig. 8 Site plan of Peng-cheng electric power plant (unit: m)

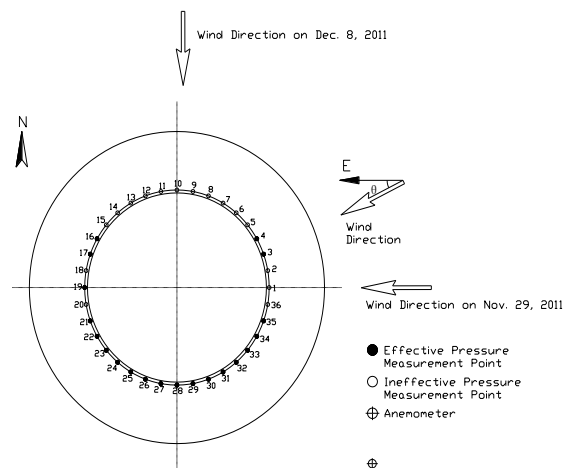


Fig. 9 Plan of pressure measurement points

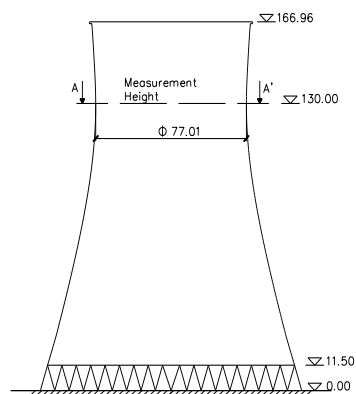
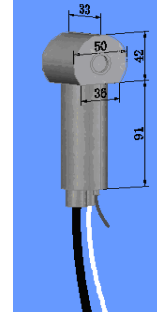


Fig. 10 Projection of measuring tower (unit: m)



(a) An actual transducer

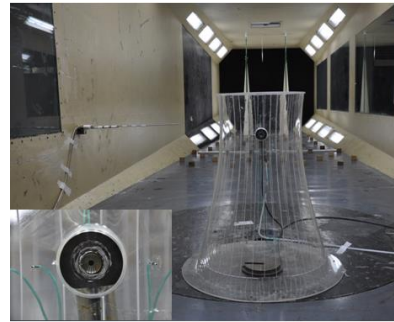


(b) Dimension (unit: mm)

Fig. 11 Wind pressure transducer

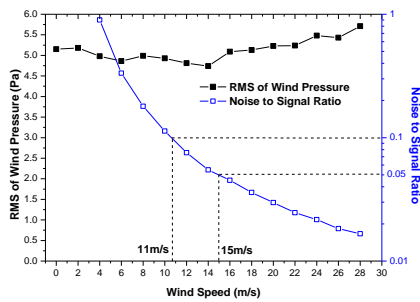


(a) Test in uniform flow field

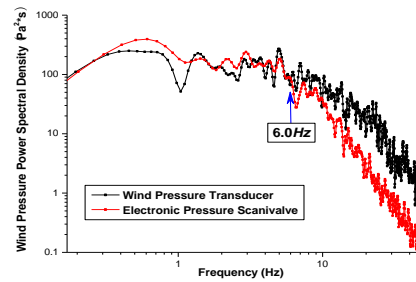


(b) Test in turbulent flow field

Fig. 12 Transducer's precision tests in TJ-2 wind tunnel



(a) Static performance



(b) Dynamic performance

Fig. 13 Test results for transducer's precision

Wind pressure transducers applied are commercially-available ones whose dimensions are: 13 cm in length, 5 cm in width, 3 cm in depth (see Fig. 11). The transducer's measuring range is from 0 to ± 2.5 kPa. Its maximum sampling frequency and precision are 100 Hz and 1/1000 maximum range, respectively.

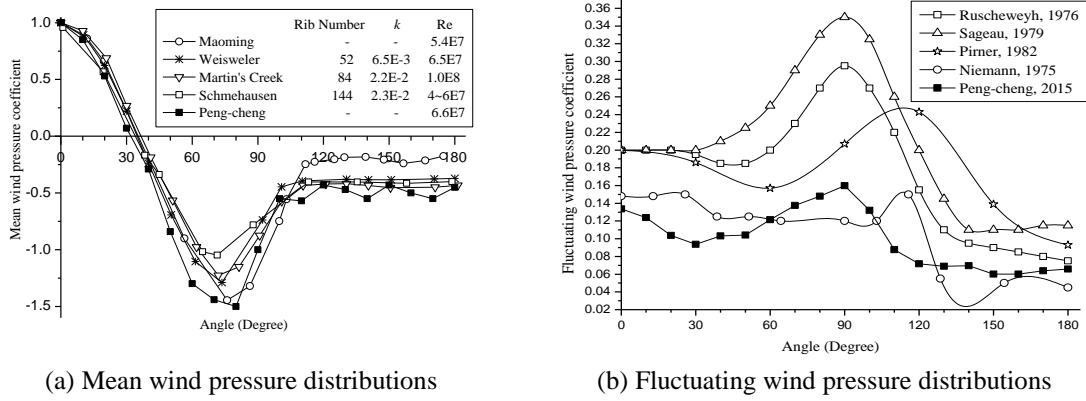


Fig. 14 Field measurement results on Peng-cheng and other cooling towers

Before installed on the prototype tower, the transducer is tested in two flow fields simulated in TJ-2 wind tunnel of Tongji University for its precision (see Fig. 12). It is found that when oncoming flow speed is greater than 15m/s, the noise to signal ratio for the transducer is kept below 5% (see Fig. 13(a)). Besides, it is shown that the signal produced by the transducer agrees with those obtained using high-precision electronic pressure scanivalve in 0-6 Hz frequency domain (see Fig. 13(b)). These prove that both static and dynamic performances of the transducer are satisfactory in time and frequency domains of interest (Zhao, Cheng *et al.* 2012).

3.2 Simultaneously measured mean and fluctuating wind pressure distributions

Although transducers are arranged around the full-circle of the tower's throat section, some transducers on the north surface were unfortunately damaged during the tower's construction. As shown in Fig. 9, only 20 out of the 36 pressure transducers are finally proved to be effective. As a result, only strong wind events with right flow directions can be utilized (e.g., that occurred on Nov. 29, 2011 in Fig. 9), and those without right flow directions fail to provide opportunities for obtaining complete half-circle full-scale data (e.g., that occurred on Dec. 8, 2011 in Fig. 9). From June, 2010 to June, 2012, several occasions of strong ABL wind scenarios with right flow directions have been observed on the site, and the wind pressure time histories produced by all transducers around the test section at those times are simultaneously recorded. The data are then processed following some steps: First, Eq. (2) is used to produce dimensionless pressure coefficients taking the wind pressure at the stagnation point as the total reference pressure and the pressure produced by a transducer at 30 degree as the static reference pressure; Second, the long-term records are divided into many 10-min data segments, and Eqs. (3) and (4) are applied to each data segment to produce many mean/fluctuating wind pressure distributions; Third, after obviously erroneous points on all the curves (e.g., those produced by transducers 18 and 20 in Fig. 9) are replaced by linear interpolated values from neighboring data, averaging is done to some selected typical mean/fluctuating wind pressure distributions. A set of resultants is obtained accordingly and presented in Fig. 14. Resultants of previous full-scale measurement campaigns in history are also shown by Fig. 14. A comparison of all the measured fluctuating wind pressure distributions in Fig. 14(b) indicates that the dynamic Re effects simulation targets for different

cooling towers vary noticeably. The discrepancies might be caused by the differences in surface roughness and incoming flow characteristics among various cooling towers.

3.3 Selections of the candidate simulation cases and the optimum simulation case

Comparing the mean wind pressure distribution measured on Peng-cheng cooling tower with the results of all 32 cases in Fig. 4(a) finds that five results are consistent with the field results, i.e., four-layer paper tape with + 6 m/s, 8 m/s, 10 m/s and 12 m/s wind speeds, and three-layer paper tape with a + 12 m/s wind speed (see Fig. 15(a)). So, they are selected as the candidate simulation cases. The mean wind pressure distributions obtained using the candidate simulation cases are basically the same as that of Peng-cheng cooling tower, but there are significant variations between most simulated fluctuating wind pressure distributions and the measured one (see Fig. 15 (b)), exhibiting the deficiency of the traditional method which ignores the truth of the simulated fluctuating wind pressure distribution.

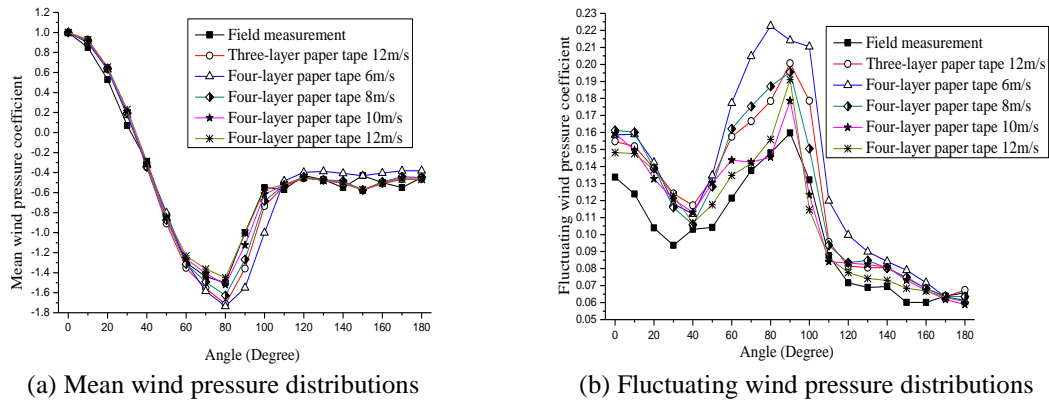


Fig. 15 Candidate simulation cases

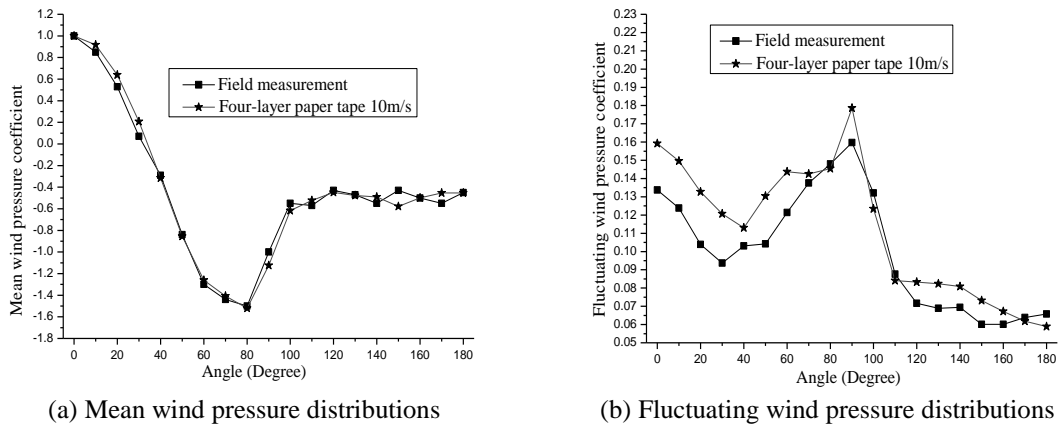


Fig. 16 Optimum simulation case

Comparing the fluctuating wind pressure distributions of the candidate simulation cases to that of Peng-cheng cooling tower (see Fig. 15(b)), it is found that, for both mean and fluctuating wind pressure distributions, the optimum high Re effects simulation case is a model with four-layer paper tape and a + 10 m/s wind speed. According to Fig. 16(a), the mean wind pressure distribution of the optimum simulation case overlaps the results of the field measurements. There is a slight difference between the simulated fluctuating wind pressure distribution and the full-scale one (see Fig. 16(b)).

4. Validations of the proposed method

Additional efforts are made to validate the proposed comprehensive high Re effects simulation method, including: (1) comparing the full dynamic properties of the simulated pressure fields with those of the full-scale one; and (2) comparing the cooling tower's dynamic structural responses obtained using the simulated wind pressure fields with the results using the real field.

For comparison, three fluctuating wind pressure fields with the duration of 60 s are used. One is obtained using the wind tunnel model tests employing the optimized parameters (hereinafter referred to as the simulated load case using the proposed method). A second one is obtained using wind tunnel tests employing four-layer paper tape + a 6 m/s wind speed simulation parameters (hereinafter referred to as the simulated load case using the traditional method). A third one is based on the field measurements conducted on Nov. 29, 2011 (hereinafter referred to as the full-scale load case).

4.1 Full covariance matrix and cross-spectral densities

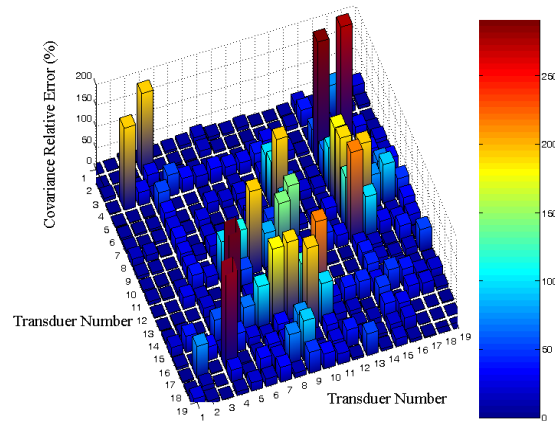
The idealized simulation state in wind tunnels should reveal the full dynamic properties of the full-scale wind pressure field, including the full covariance matrix and the cross-spectral densities, which are indispensable for obtaining the structural dynamic responses. First, the full covariance matrices of the simulation cases are compared with the real case. The relative error between simulated and full-scale covariance is defined as:

$$\delta = \frac{|C_s - C_F|}{C_F} \times 100\% \quad (5)$$

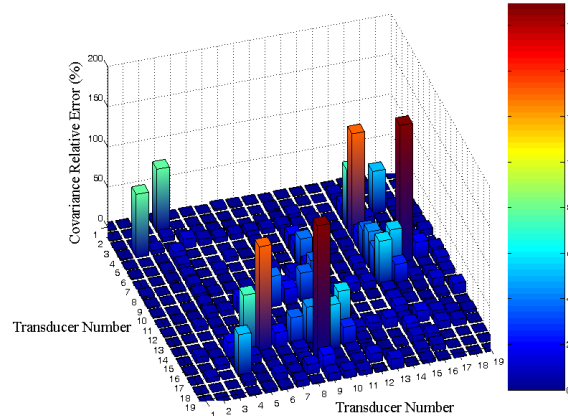
where C_s and C_F are simulated covariance and full-scale covariance, respectively. Fig. 17(a) shows the relative errors calculated for the traditional method. As can be seen, some relative errors are larger than 150%, which demonstrates that the idealized simulation state is not achieved using the traditional method. On the contrary, almost all the calculated covariance relative errors for the proposed method are smaller than 50%, as is shown in Fig. 17(b).

Second, the cross-spectral densities of the simulation cases are compared with the full-scale case. In Figs. 18(a), 18(c) and 18(e), notable underestimations of the cross-spectral densities are found over the full frequency range for simulated pressures using the traditional method at windward, side and wake locations. This is probably caused by the low coherence between the simulated pressures. In Figs. 18(b), 18(d), 18(f), the cross-spectral densities for pressures simulated using the proposed method agree well with the real values at all locations.

Comparisons of the dynamic properties of the wind pressure fields demonstrate the superiority of the proposed method. However, it should be admitted that a few errors for the simulation results using the proposed method are still notable, and the discrepancies are probably caused by (1) the inadequate simulation of large-scale turbulence content in ABL in the wind tunnel; (2) the differences in stationary states of the wind flow for the two cases; and (3) the Jensen number effects. To be specific, the geometric scaling for a model test is not necessarily determined by the turbulence integral length measured in a wind tunnel. The appropriate scaling for TJ-3 is around 1:400~1:300. However, the scaling required for our test is 1:200. So the scale of turbulent content simulated in the wind tunnel might be smaller than the correct value. Besides, full-scale ABL wind velocity fields lack stationarity as compared with the wind tunnel situations (Dalglish 1969). The full-scale wind velocity and the full-scale wind direction are sometimes unsteady (Cheng, Zhao *et al.* 2015), which can hardly be simulated in a passive wind tunnel. The third, the roughness length of the flow simulated in a wind tunnel is sometimes not correctly scaled according to the geometrical scaling, inducing the Jensen effects. All of these can cause discrepancies between full-scale and model test results.

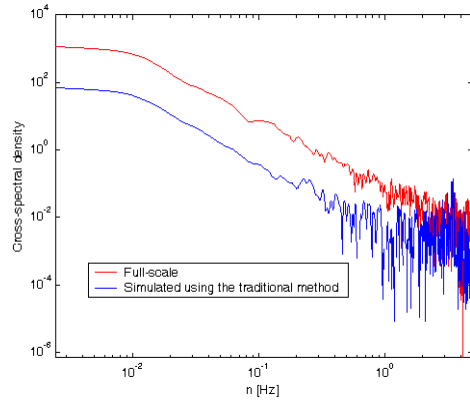


(a) Relative errors for simulated covariance using the traditional method

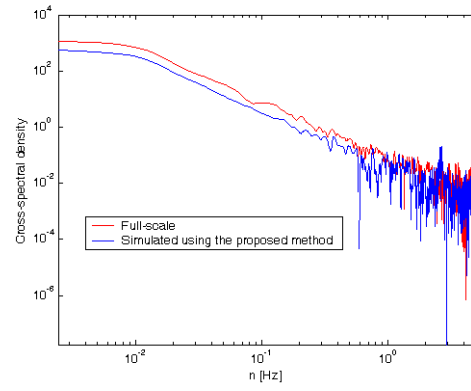


(b) Relative errors for simulated covariance using the proposed method

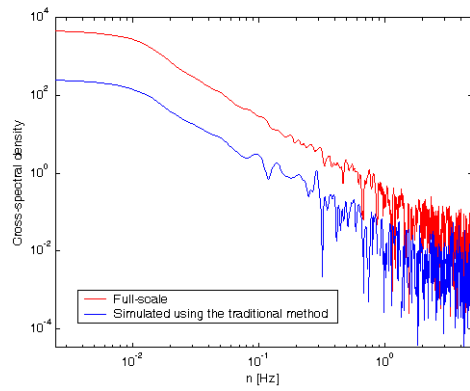
Fig. 17 Relative errors between simulated and full-scale covariance (transducers 1, 2, ..., 19 refer to those located at the positions with 0° , 10° , ..., 180° included angles from the stagnation point)



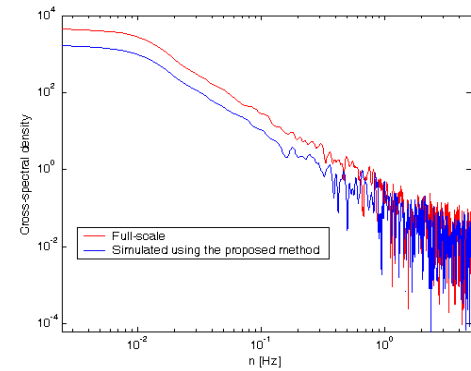
(a) Transducer 3-4 (traditional method)



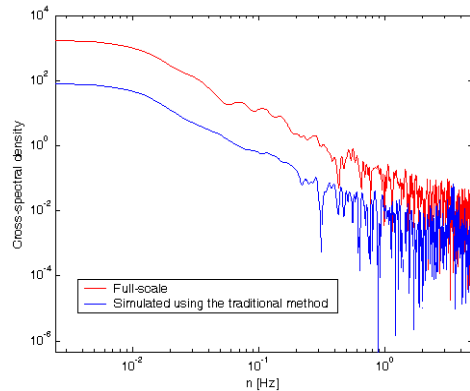
(b) Transducer 3-4 (proposed method)



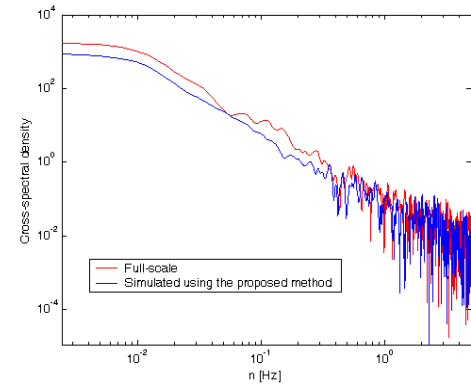
(c) Transducer 10-12 (traditional method)



(d) Transducer 10-12 (proposed method)



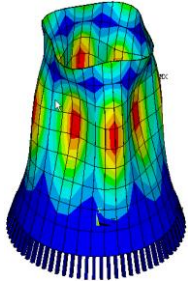
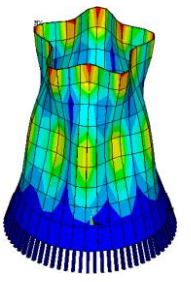
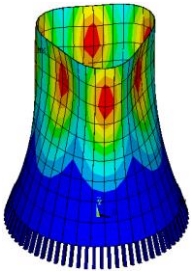
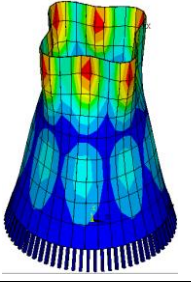
(e) Transducer 15-16 (traditional method)



(f) Transducer 15-16 (proposed method)

Fig. 18 Simulated and full-scale cross-spectral densities for windward, side and wake pressures

Table 4 Natural frequency and vibration shape of cooling tower

Mode	Frequency (Hz)	Mode shape (circumferential /meridian harmonic wave numbers)	View of mode shape	Mode	Frequency (Hz)	Mode shape (circumferential /meridian harmonic wave numbers)	View of mode shape
1	0.738	4/1		3	0.748	5/2	
2	0.745	3/1		4	0.782	4/2	

4.2 The cooling tower's responses to wind pressure fields

4.2.1 Finite element analyses

A 250 m high cooling tower is modeled by discrete spatial shell elements using a commercially-available finite element (FE) software. The FE model comprises 324 shell elements. 36 pairs of herringbone columns with fixed bottom ends are modeled by spatial beam elements. The total weight of the tower is 175180 t, and its 1st~4th dynamic properties are listed in Table 4.

For all the three load cases, only wind pressure data at the throat section of the cooling tower are used for the analyses. Fluctuations of wind pressure coefficients at other heights are assumed to be identical to those of the throat section, so data for the whole surface are obtained (a similar assumption was made by Basu and Gould (1980) for calculating cooling towers' dynamic responses to wind fluctuations).

A time domain approach Newmark- β method is used for calculating the structural dynamic responses. The results for the three load cases are compared with each other to examine the proposed method. With a 1:200 length scaling for the wind tunnel model and the velocity used in the wind tunnel setting a velocity scaling ($\approx 1:1$), a time scaling 1:200 is set whereby the phenomena of interest occurs faster in the wind tunnel than at full-scale. So when calculated structural responses for Peng-cheng tower are compared to those for load cases derived from wind tunnel modeling, the latter are adjusted to account for the time scaling.

4.2.2 Analyses results

Using the full-scale load case, the analysis for structural dynamic time-history response is conducted. The sum displacement for the whole cooling tower at 0.8 s is shown by Fig. 19. As shown in Fig. 19, the deformation shape featured a sagging-inward windward region and a bowing-outward sideward region (the red areas in the nephogram). Fig. 19 is only a picture of the structure's response at one moment within the 60 s duration. In reality, the tower response changes over time.

Using the simulated load cases, analyses are performed in the same way and the dynamic structural responses are obtained accordingly. Fig. 20 compares the results of the full-scale load case and the simulated load case using the traditional method. From Figs. 20(a) and 20(c), the mean values of the time history curves for the two load cases appear to be similar in the windward and wake regions. But the discrepancy of the mean values is notable in the side region (see Fig. 20 (b)). Although the variation trends are similar, all the oscillation amplitudes of the simulated load case are greater than those of the full-scale load case at all times. This clearly shows the deficiencies of the traditional Re effects simulation method.

Furthermore, Figs. 21(a)-21(c) compares the structural displacement time histories obtained for the simulated load case using the proposed method to those for the full-scale load case. Obviously, both the mean values and the oscillation amplitudes of curves for the two load cases are close at all surface points.

Fig. 22(a) compares the mean displacements for the two simulated load cases with those for the full-scale load case at locations around the cooling tower's throat section. There is little difference between the values for the simulated case using the traditional method and the full-scale values. However, in Fig. 22(b), the displacement standard deviations of the simulated load case using the traditional method are much greater than those of the full-scale load case around the half-circle.

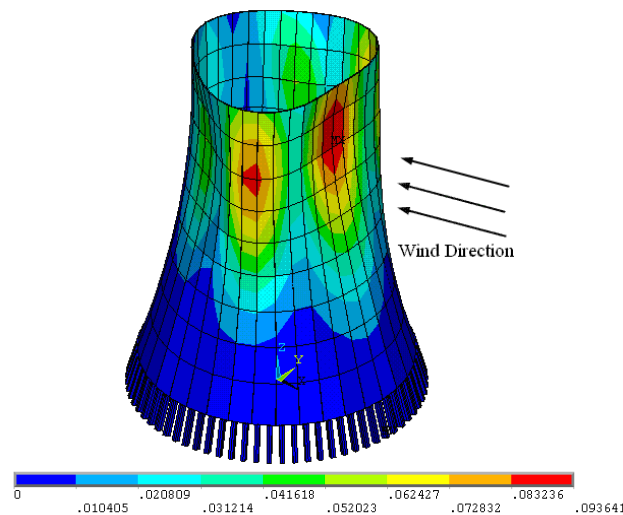
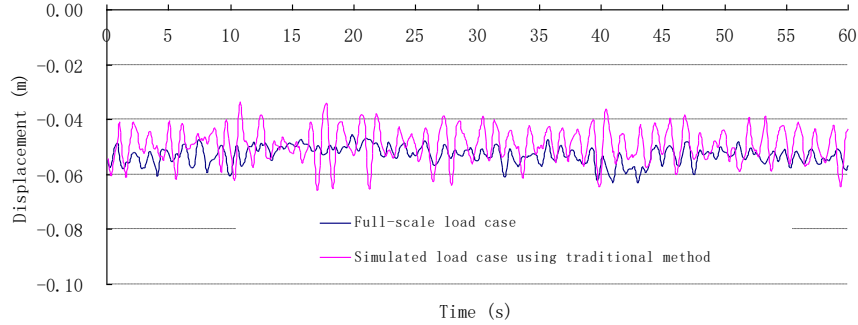
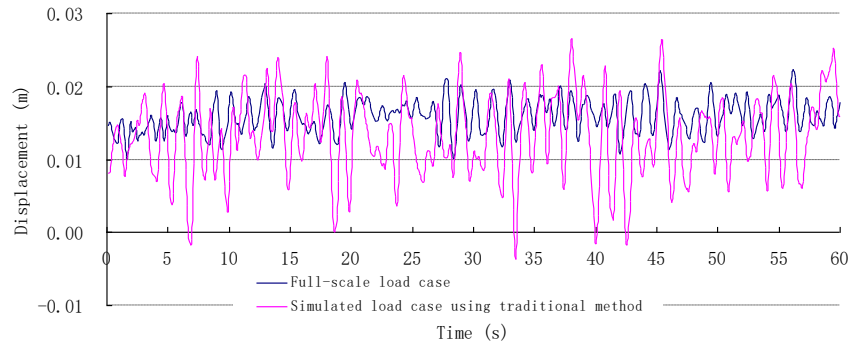


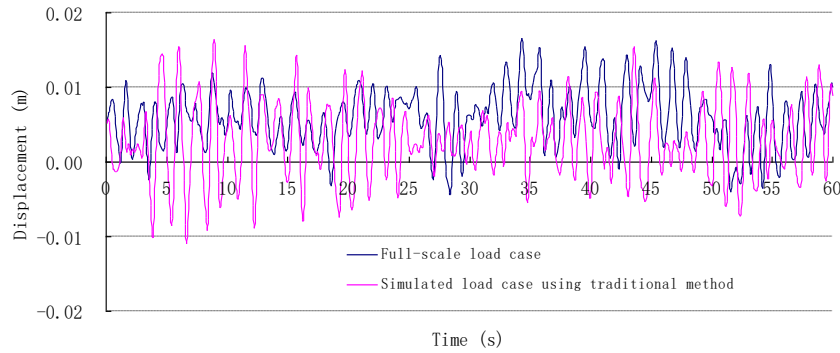
Fig. 19 Displacement vector sum for the whole cooling tower using full-scale load case at 0.8s (unit: m)



(a) Circumferential position: 0 degree



(b) Circumferential position: 90 degree



(c) Circumferential position: 180 degree

Fig. 20 Radial displacement time-histories for full-scale load case and simulated load case using the traditional method

On the whole, the structural responses for the full-scale load case and the simulated load case using the traditional method agree well with respect to the mean displacements (25.14% relative error in average), but they fail to reach such agreement considering the standard deviations of the displacements (90.17% relative error in average). However, the agreement between the full-scale load case and the simulated load case using the proposed method is much better with respect to both the mean and the standard deviation of the structural responses (17.88% average relative error for mean displacements and 25.05% average relative error for displacement standard deviations).

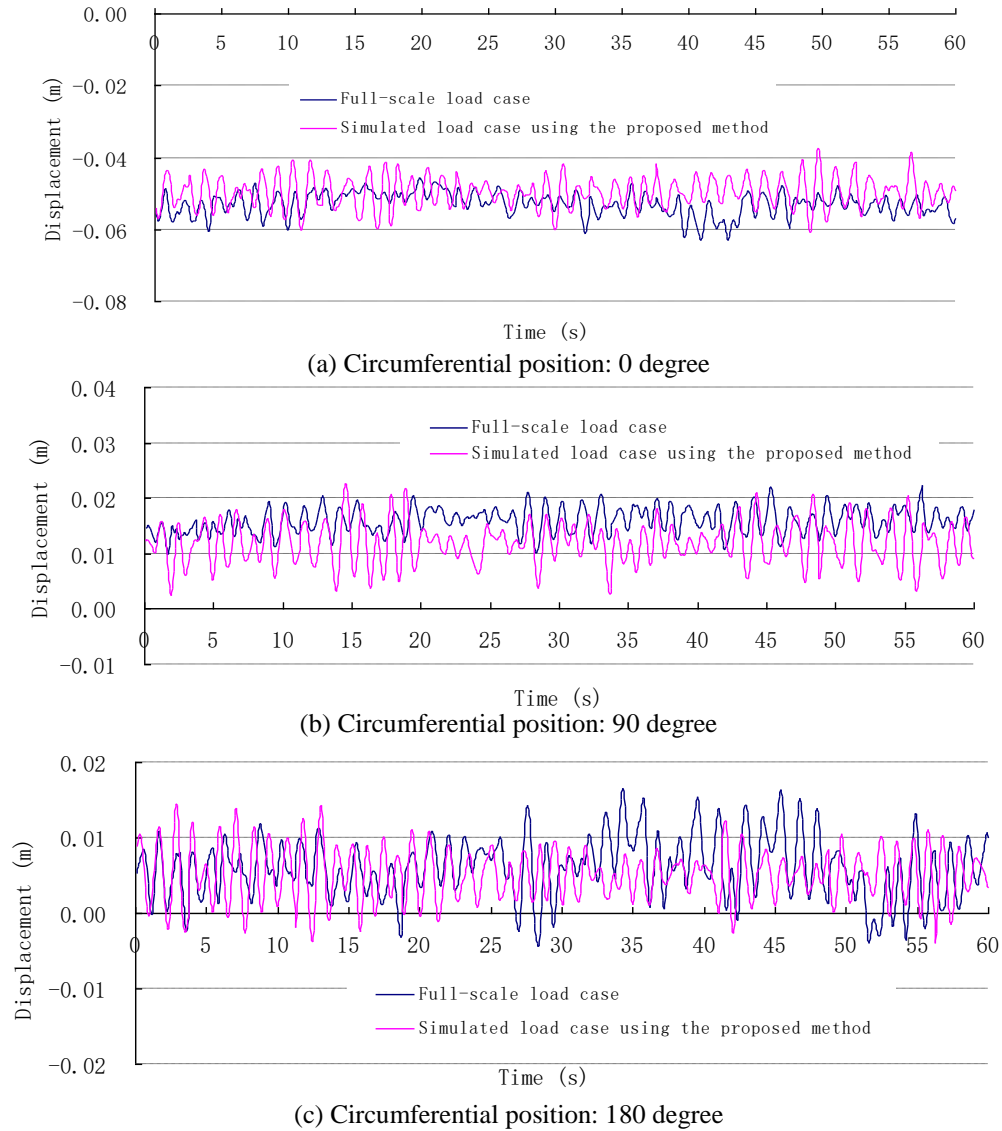


Fig. 21 Radial displacement time-histories for full-scale load case and simulated load case using the proposed method

5. Conclusions

This study finds that the comprehensive Re effects simulation method is more reliable than the traditional simulation method for use in wind tunnel cooling tower model tests. Based on in-depth study of the surface roughness effects on the mean/fluctuating wind pressure distributions on cooling towers, a comprehensive simulation method is conceived. Through a case study, this work presents the proposed method which consists of the following. First, simulation cases are obtained as many as possible by varying the surface roughness of the model and the applied wind speed.

Among these cases is a small group which can correctly produce the mean wind pressure distribution at a high Re. Then, the optimum simulation case is selected from this small group by comparing the simulated fluctuating wind pressure distributions with the values measured in the field for the full-scale cooling tower.

The proposed method is then tested for its effectiveness. This consists of first, the simulated full covariance matrices and cross-spectral densities are compared with those of the full-scale case and the results show that it is possible to replicate the full dynamic properties of the full-scale wind pressure field in the wind tunnel using the proposed simulation method. Second, the cooling tower's structural responses obtained using the simulated wind pressure fields are compared with those using the full-scale field. It is found that the dynamic responses obtained for the simulated load case using traditional method are much greater than those obtained for the full-scale load case. But the results for the simulated load case using the proposed method agree well with those for the full-scale load case with respect to both static and dynamic responses. The superiority of the proposed method is thereby validated.

Another comprehensive high Re effects simulation method is also mentioned in Sec. 2.3. It employs more influences (the surface roughness and the turbulence intensity), and an active control wind tunnel is required for that method.

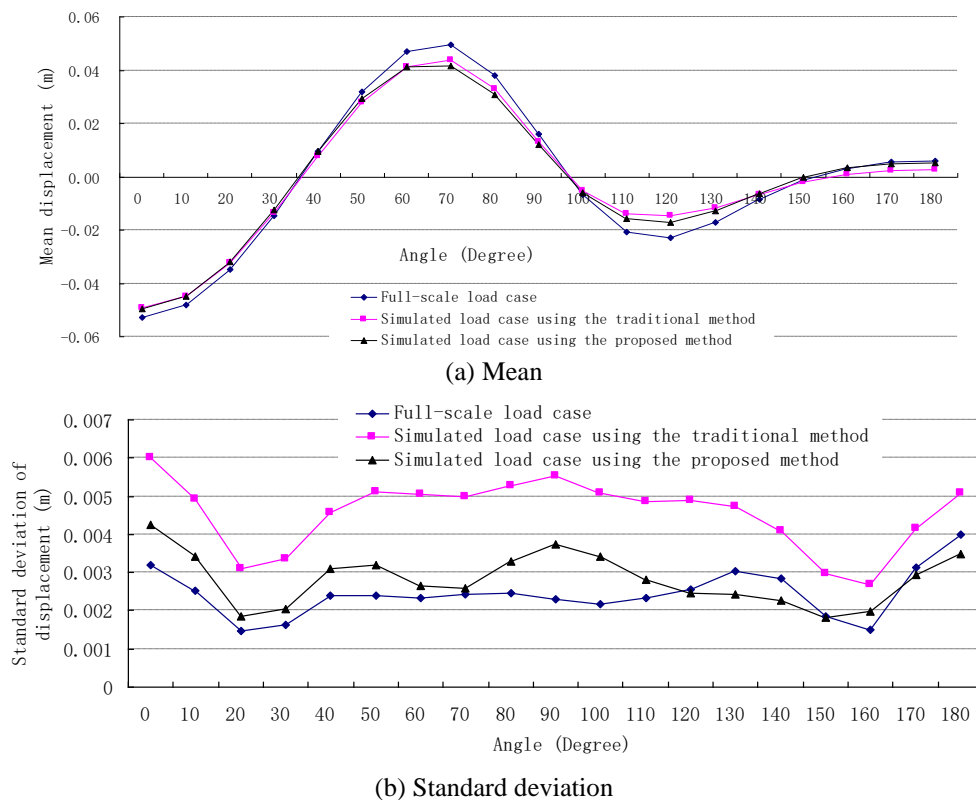


Fig. 22 Displacements around the throat section

Finally, it should be noted that any high Re effects simulation method requires field measurement results as targets. The existing field measurement results shared by the wind

engineering community are still limited, and they can only be applied to individual occasions. In this regard, long-term full-scale measurements on Peng-cheng cooling tower should continue and our new full-scale measurement campaigns will be launched in the future to obtain first-hand data on towers of different surface roughness and under various types of incoming flows. Then works should be carried out to generalize and formulate the relationship between the influences (i.e., the Re , the surface roughness and the turbulence intensity) and the full-scale static/dynamic wind effects, so that full-scale measurements are no longer necessary. Besides, the proposed method requires additional substantial validation in the future. This is because more work is needed to prove that the proposed method can work out as well as is demonstrated in this paper for cooling towers with parameters different from those of Peng-cheng tower. In application, we concern more about the simulation of fluctuating wind pressure distribution, rather than the simulation of mean wind pressure distribution. This is because the full-scale mean wind pressure distributions obtained to this day are similar (see Fig. 14(a)), and it has been proved that they can be accurately simulated in the wind tunnel. However, the full-scale fluctuating wind pressure distributions are widely variable (see Fig. 14(b)). When the candidate simulation cases are obtained using the proposed method, we are not sure that one can fortunately get one case within the limited candidate simulation cases whose fluctuating wind pressure distribution happens to overlap the unpredictable target. Anyway, it has already been a step forward that the truth of the simulated fluctuating wind pressure distribution is taken into account in our proposed method. For the traditional simulation method, the realness of the dynamic wind effects obtained is a critical issue.

Acknowledgements

The authors gratefully acknowledge the support of the National Natural Science Foundation of China (51178353 and 51222809) and the National Key Basic Research Program of China (i.e. 973 Program) (2013CB036300), and the support of the Kwang-Hua Fund for the College of Civil Engineering, Tongji University.

References

- Achenbach, E. (1968), "Distribution of local pressure and skin friction around a circular cylinder in cross-flow up to $Re=5 \times 10^6$ ", *J. Fluid Mech.*, **34**, 625-639.
- Basu, P.K. and Gould, P.L. (1980), "Cooling tower using measured wind data", *J. Struct. Division - ASCE*, **106**, 579-600.
- Bearman, P.W. (1969), "On vortex shedding from a circular cylinder in the critical Reynolds number regime", *J. Fluid Mech.*, **34**, 577-585.
- Cheng, X.X., Zhao, L., Ge, Y.J., Ke, S.T. and Liu, X.P. (2015), "Wind pressures on a large cooling tower", *Adv. Struct. Eng.*, **18**(2), 201-220.
- Dalglish, W.A. (1969), "Experience with wind pressure measurements on a full-scale building", *Proceedings of the technical meeting concerning wind loads on buildings and structures*. Gaithersburg, Maryland.
- Farell, C. and Blessmann, J. (1983), "On critical flow around smooth circular cylinders", *J. Fluid Mech.*, **136**, 375-391.
- Kargarmoakhar, R., Chowdhury, A.G. and Irwin, P.A. (2015), "Reynolds number effects on twin box girder
- Lawson, T.V. (1982), "The use of roughness to produce high Reynolds number flow around circular

- cylinders at lower Reynolds numbers”, *J. Wind Eng. Ind. Aerod.*, **10**, 381-387.
- Lee, S., Kwon, S.D. and Yoon, J. (2014), “Reynolds number sensitivity to aerodynamic forces of twin box bridge girder”, *J. Wind Eng. Ind. Aerod.*, **127**, 59-68.
- Ma, W.Y., Liu, Q.K., Du, X.Q. and Wei, Y.Y. (2015), “Effect of the Reynolds number on the aerodynamic forces and galloping instability of a cylinder with semi-elliptical cross sections”, *J. Wind Eng. Ind. Aerod.*, **146**, 71-80.
- Ministry of Energy, P.R.C. (1989), NDGJ5-88: Technical Specification for Hydraulic Design of Thermal Power Plant.
- Niemann, H.J. (1971), *Zur stationären windbelastung rotations symmetrischer Bauwerke im Bereich transkritischer Reynoldszahlen*, Mitt. Nr. 71-2, Tech.-wissensch. Mitt., Institut für Konstr. Ing.-ban, Ruhr-Universität Bochum, West Germany.
- Niemann, H.J. and Hölscher, N. (1990), “A review of recent experiments on the flow past circular cylinders”, *J. Wind Eng. Ind. Aerod.*, **33**(1-2), 197-209.
- Niemann, H.J. and Propper, H. (1975, 1976), “Some properties of fluctuating wind pressures on a full-scale cooling tower”, *J. Ind. Aerod.*, **1**, 349-359.
- Niemann, H.J. and Ruhwedel, J. (1980), “Full-scale and model tests on wind-induced, static and dynamic stresses in cooling tower shells”, *Eng. Struct.*, **2**, 81-89.
- Pan, T., Zhao, L., Cao, S.Y., Ge, Y.J. and Ozono, S. (2011), “Analysis of aerodynamic load effect on thin plate section in multiple fan active control wind tunnel”, *Procedia Eng.*, **14**, 2481-2488.
- Pirner, M. (1982), “Wind pressure fluctuations on a cooling tower”, *J. Wind Eng. Ind. Aerod.*, **10**, 343-360.
- Qiu, Y., Sun, Y., Wu, Y. and Tamura, Y. (2014a), “Effects of splitter plates and Reynolds number on the aerodynamic loads acting on a circular cylinder”, *J. Wind Eng. Ind. Aerod.*, **127**, 40-50.
- Qiu, Y., Sun, Y., Wu, Y. and Tamura, Y. (2014b), “Modeling the mean wind loads on cylindrical roofs with consideration of the Reynolds number effect in uniform flow with low turbulence”, *J. Wind Eng. Ind. Aerod.*, **129**, 11-21.
- Roshko, A. (1961), “Experiments on the flow past a circular cylinder at very high Reynolds number”, *J. Fluid Mech.*, **10**(3), 345-356.
- Ruscheweyh, H. (1975/1976), “Wind loadings on hyperbolic natural draft cooling towers”, *J. Ind. Aerod.*, **1**, 335-340.
- Sollenberger, N.J. and Scanlan, R.H. (1974), “Pressure-difference measurements across the shell of a full-scale natural draft cooling tower”, *Proceedings of the Symposium on Full-scale Measurements of Wind Effects*, University of Western Ontario, Canada.
- Sun, T. and Zhou, L. (1983), “Wind pressure distribution around a ribless hyperbolic cooling tower”, *J. Wind Eng. Ind. Aerod.*, **14**, 181-192.
- Wang, X. and Gu, M. (2015), “Experimental investigation of Reynolds number effects on 2D rectangular prisms with various side ratios and rounded corners”, *Wind Struct.*, **21**(2), 183-202.
- Zhao, L., Cheng, X., Dong, R. and Ge, Y. (2012), “Investigation of surface roughness and its influence to flow dynamic characteristics of hyperbolic cooling tower”, *Proceedings of the 6th International Symposium on Cooling Towers*, Cologne, Germany.